DEPRESSED COLLECTORS FOR A LARGE ORBIT GYROTRON*

A. Singh, D. Goutos, W.R. Hix, W. Lawson, C.D. Striffler,
V.L. Granatstein, and W.W. Destler

Laboratory for Plasma and Fusion Energy Studies
University of Maryland, College Park, MD 20742

ABSTRACT

An auxiliary magnetic cusp transforms rotational motion in the spent beam of a Large-Orbit Gyrotron into axial motion. Results regarding the interfacing of this cusp with a depressed collector region and the effects of the magnetic field profile together with collector geometry and potentials on energy sorting are discussed.

INTRODUCTION

In the case of spiraling beam devices, rotational motion in the spent beam needs to be converted into axial motion before its energy can be transferred to the axial retarding fields of depressed collectors.The axis encircling beam in a large-orbit gyrotron may be generated by passing an axially streaming beam through a magnetic cusp. After rf interaction the spent beam can be "unwound" by passing through a second cusp having a reversed orientation of the magnetic field.[1] An important factor representing this effect is the ratio of the perpendicular component to the axial component of velocity, denoted by α. This factor has been studied in the region between the two cusps as well as after the second cusp.[2] The residual α in the latter region is typically a small fraction of the midrange α indicating a substantial conversion of rotational to axial energy.

The parameters of the depressed collector region are the subject of the present study. Their effect on energy sorting among different depressed collectors and estimates of collector efficiency for two configurations are presented.

THE SYSTEM

A schematic diagram of the large orbit gyrotron and an energy recovery system is shown in Fig.1. The Pierce gun that precedes the first cusp, the rf interaction region between the two cusps, and the depressed collector region that follows the second cusp are indicated. Also shown is a typical profile of the magnetic field. It is generated by coils in the three regions. Two iron plates with annular rings cut out from them, form the two cusps. The first one generates the axis-encircling beam, and the second one unwinds it.

The parameters for the gun and the cusps were optimized in an earlier study[2] and are compatible with the cusptron experiment at the University of Maryland.[3] The cathode voltage is 26 kV, balanced cusp magnetic field strength is ~ 330 G, half widths of the cusps are 4 mm and 10 mm respectively, radial extent of the cathode as well as the beam aperture associated with the first cusp is 1.4 cm to 1.6 cm, radial extent of the beam aperture of the second cusp is 1.0 to 2.0 cm, and the distance between the midpoints of the two cusps is 30 cm.

SIMULATION OF TRAJECTORIES AND MODELLING OF ENERGY CHANGES

The path of the particles through the two cusps is simulated using a single particle code.[2] The radii and angles at which they emerge from the second cusp into the collector region are used as inputs to the Herrmannsfeldt code,[4] which determines the trajectories in the collector region. As a first approximation of the transfer of energy to the rf field, a change in the transverse energy of the beam electrons is introduced at a point between the two cusps. A Gaussian weighting factor is applied to 5 beamlets into which the beam is divided. The energy changes are taken as, -30%, -20%, -10%, 0.0%, and +10% of the initial energy of the beam. The median value of energy is 10% lower than the initial energy of the beam, corresponding to a typical electronic efficiency of 10%. The Gaussian width was varied from 1 kV to 2.6 kV. The space charge effects did not markedly change the sorting of beamlets between different collectors.

ENERGY SORTING AND SOFT-LANDING OF BEAMLETS

Figure 2 shows trajectories for 5 beamlets in the case of 2 depressed collectors at potentials of -12.5 and -20 kV. Energy sorting is seen, as beamlets of energy 28.6 keV, 26 keV and 23.4 keV are collected on the -20 kV electrode, and those of 20.8 and 18.2 keV on the -12.5 kV electrode.

Figure 3 shows a subsequent iteration with 4 depressed collectors at potentials of -5, -13, -18 and -23 kV. In this case beamlets of 28.6 keV and 26 keV energy are collected at -23 kV, those of 23.4 keV and 20.8 keV are collected at -18 kV, and those of 18.2 keV at -13 kV. Compared to the previous case, the gap between the energy of the beamlet and the electrode potential is reduced, implying greater transfer of energy to the electrostatic field and thus less to heat dissipation.

ESTIMATION OF COLLECTOR EFFICIENCY AND ITS DEPENDENCE ON VARIOUS PARAMETERS

For each beamlet the collector efficiency is given by the ratio of the collector potential to the energy of the beamlet. The overall collector efficiency η_R is calculated by applying a Gaussian weighting factor.

Trajectory simulations are carried out in the energy recovery system to study the effects caused by variations in magnetic, geometrical and electrical parameters. Their effects are interrelated. Electrode configurations used with success in linear beam tubes are a useful starting

* This work is supported by AFOSR.

CH2490-1/87/000-0389 $1.00 ©1987 IEEE

point[5] for further iterations.

The effects of magnetic field profile between the second cusp and the last collector are studied. The magnetic field is generated by two coils in the collector region, one near the second cusp and the other near the last collector. The latter partially cancels the effect of the former. The field profile is also included in the Herrmannsfeldt code simulations. The location and current of each coil could be varied to get the desired profile. An important criterion is avoidance of reflection of any electrons at an intermediate stage. Too large an end field, coupled with too high a negative potential on the electrodes, tend to cause such reflections. Too small an end field results in expansion of even the highest energy particle trajectories to the peripheral electrodes. A residual magnetic field at the last collector an order of magnitude lower than at the second cusp is found to be useful in energy sorting, keeping the highest energy beamlets to smaller radii.

The effects due to electrode geometry and potentials are studied in relation to the axial location of the collectors and their radial dimensions. Too short a gap between the second cusp and the first depressed collector tends to cause reflections. The radial dimension however, could be successfully reduced by 20% in the iteration. Assuming a spread in the Gaussian distribution of 1.85 kV, the estimated collector efficiency for 2 depressed collectors is of the order of 72% and that for 4 depressed collectors of the order of 80%. It is to be noted that a collector efficiency of 80% in tandem with an electronic efficiency of 10% yields an overall device efficiency of 36%.

CONCLUSIONS

An auxiliary cusp in large-orbit gyrotrons converts a large percentage of the rotational energy in the spent beam into axial energy. This makes it possible to collect the different portions of the beam energy-wise on electrodes at potentials sufficiently depressed to give good collector efficiency. Estimates of this efficiency for a configuration of 4 depressed collectors are of the order of 80%, for a spent beam from a device operating at 10% electronic efficiency. This gives an attractive possibility of enhancement of overall efficiency in a large orbit gyrotron operating in a high harmonic mode.

REFERENCES

1. Amarjit Singh, E.P. Chojnacki, W.W. Destler, D. Goutos, V.L. Granatstein, W. Lawson and C.D. Striffler, Conference Record IEEE Int'l Conf. Plasma Science, Paper 2Y6, p.40, Arlington, VA, June 1987.

2. A. Singh, W. Lawson, D. Goutos, W.R. Hix, C.D. Striffler, V.L. Granatstein and W.W. Destler, Int. J. Electronics (submitted for publication).

3. E. Chojnacki, W.W. Destler, W. Lawson and W. Namkung, J. Appl Phys. 61 (4), 1268-1275, (1987).

4. W.B. Herrmannsfeldt, "Electron Trajectory Programs," SLAC Report 226, Nov. 1979.

5. E.W. McCune, Technical Digest, IEDM, 160-163, (1986).

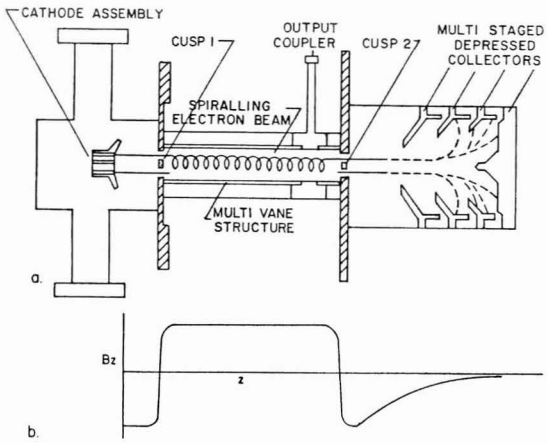

Fig. 1a. Schematic diagram of a large orbit gyrotron with depressed collectors
1b. Typical magnetic field profile

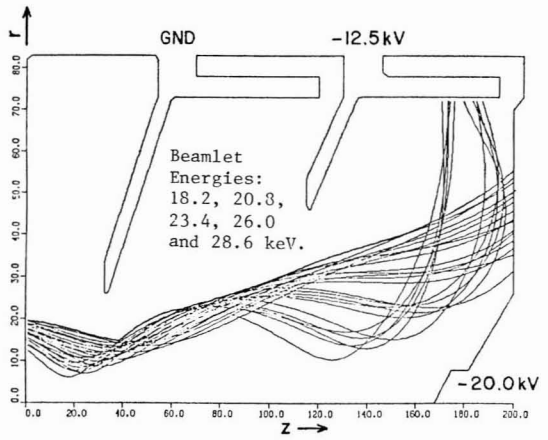

Fig. 2 Trajectories for two depressed collectors (different scales for z and r in mm)

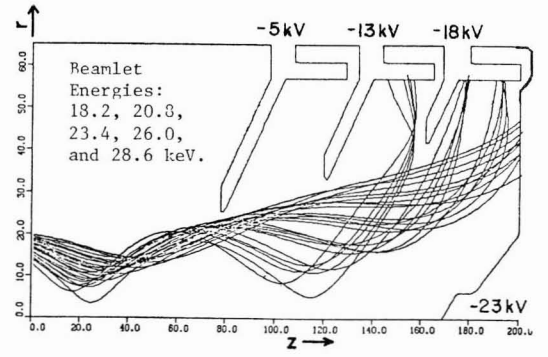

Fig. 3 Trajectories for four depressed collectors (different scales for z and r in mm)